Interval Observer-Based Controller Design for Systems with State Constraints: Application to Solid Oxide Fuel Cells Stacks

Sara Ifqir, Andreas Rauh, Julia Kersten, Dalil Ichalal, Naïma Aït Oufroukh, Saïd Mammar

Interval Observer-Based Controller Design for Systems with State Constraints: Application to Solid Oxide Fuel Cells Stacks

Sara Ifqir[1], Andreas Rauh[2], Julia Kersten[2], Dalil Ichalal[1], Naima Ait-Oufroukh[1] and Said Mammar[1]
[1]IBISC Laboratory, Univ. Evry, Paris-Saclay University, Evry, 91020, France
Email: {Sara.Ifqir, Dalil.Ichalal, Naima.Aitoufroukh, Said.Mammar}@univ-evry.fr
[2]Chair of Mechatronics, University of Rostock, D-18059 Rostock, Germany
Email: {Andreas.Rauh, Julia.Kersten}@uni-rostock.de

***Abstract*—For many practical applications, it is necessary to design controllers that are, one the one hand, robust against bounded uncertainty in selected parameters and external disturbances. On the other hand, it is also quite common for such systems, that state constraints need to be accounted for which must not be exceeded for any possible parameter value. Although the task is quite challenging, several robust control design procedures were designed in recent years which allow for solving these problems, especially with respect to the latter aspect. In this paper, such robust control procedures are combined in a novel manner with an interval observer to additionally handle the influence of unknown but bounded measurement noise and to prevent the violation of state constraints in a provable fashion.**

I. Introduction

Interval observers have been developed in recent years for several dynamic systems which are described by either finite-dimensional sets of state equations or (parabolic) partial differential equations [3], [4], [7], [9]. In all cases, the design of these observers makes use of the derivation of suitable bounding systems which allow for the computation of guaranteed lower and upper state bounds despite set-valued uncertainty in system parameters, bounded external disturbances, and bounded (usually additive) measurement noise.

The computation of guaranteed lower and upper bounds for such estimates commonly relies on the system property of cooperativity which leads to a specific ordering relation in the following form: Lower and upper bounding systems can be described by independent sets of state equations [15], where each of them depends on selected extremal parameter combinations. Such independence can be achieved (for linear finite-dimensional dynamics), if the system matrix is Metzler, i.e., it consists only of non-negative off-diagonal elements [6].

Such models are widely applicable in many disciplines of engineering, especially from the field of thermo-fluidic systems. To make a feedback controller for such cooperative systems robust against bounded uncertainty, it is desired that the error dynamics of the closed control loop remains cooperative and that the worst-case influence of uncertain parameters and bounded noise can be forecasted in a rigorous manner. Bounded noise usually influences the closed-loop dynamics implicitly via tolerance bounds for the state variables that are reconstructed by a model-based state observer.

This paper aims at designing robust interval observer-based state feedback controllers for cooperative systems given in the above-mentioned cooperative form so that besides insensitivity against uncertainty, the violation of user-defined upper state bounds is prevented with certainty.

Sec. II gives a brief overview of the task of temperature control for solid oxide fuel cells (SOFCs) for which the class of cooperativity-preserving robust controllers with state constraints is of huge practical relevance. The robust control design problem is solved in Sec. III by means of a novel linear matrix inequality (LMI) approach for the combined interval observer and cooperativity-preserving control synthesis. Sec. IV summarizes representative simulation results for a mathematical model of the thermal behavior of an SOFC stack module which is parameterized on the basis of measured data gathered on a test rig available at the Chair of Mechatronics at the University of Rostock. Finally, conclusions and an outlook on possible future research activities are given in Sec. V.

II. Modeling the Thermal Behavior of SOFC Stack Modules

SOFCs are typically operated at high temperature levels and provide the possibility to supply users simultaneously with thermal and electrical energy. Common applications of SOFCs can be found in the area of a decentralized power supply in which chemical energy contained in a fuel gas (such as hydrogen or hydro-carbonates) is directly converted into heat and electricity [1], [8].

In comparison with combustion engines, converting chemical energy through intermediate conversion stages into rotary mechanical energy, which is then transformed into electricity by electrical generator units, the type of energy conversion of SOFCs cells is not a-priori limited by the Carnot efficiency. Hence, significantly higher efficiency levels are, at least theoretically, possible. To exploit this advantage, it is, however, necessary to derive control strategies which prevent local overtemperatures in the interior of the SOFC stack with high reliability [12], [13]. Such overtemperatures are typically

responsible for accelerated aging of the fuel cell stack and for degradation leading to the stack's destruction in the worst case.

To derive robust control strategies and associated reliable observers, which reconstruct the cell temperature distribution in an efficient model-based way by exploiting readily available measurements (i.e., the media temperatures at the gas inlet and outlet manifolds), it is inevitable to derive low-dimensional system models in terms of sets of ordinary differential equations (ODEs). Due to the complex structure of SOFC modules and due to limited possibilities for measurement of temperatures in its interior, suitable sets of state equations contain parameter values for which only worst-case interval bounds are known [11].

Following the early lumping semi-discretization procedure summarized in [14], which exploits a spatial subdivision of the cuboid SOFC module into a finite number of $n = L \cdot M \cdot N$ elements with piecewise homogeneous temperatures in each element (cf. Fig. 1), quasi-linear state equations

$$\dot{x} = A\,(x,p) \cdot x + \tilde{B}\,(x,p) \cdot \tilde{u} \tag{1}$$

can be obtained, where the parameter vector p contained in both the system and input matrices allows for modeling of

- heat transfer due to heat conduction and convection (comprising a linearized model for heat radiation),
- enthalpy flows of the supplied gases, where χ in Fig. 1 denotes all relevant gas fractions at the anode and cathode side,
- exothermic reaction enthalpies, and
- Ohmic losses due to electric currents $I_{\mathcal{I}}$.

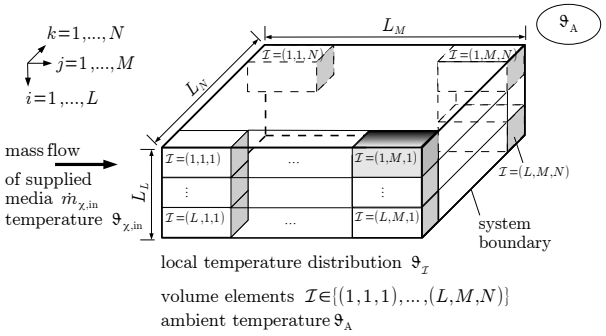

Fig. 1. Spatial semi-discretization of the fuel cell stack module.

One of the simplest, practically useful semi-discretizations is given by $L = N = 1$ with $M = 3$. This type of model approximates the SOFC stack temperature distribution in the direction of the parallel gas mass flows of both, the anode gas (i.e., the fuel gas mixture) and the cathode gas (typically preheated air). The resulting set of n ODEs is used in the following for the development of a novel interval observer-based reliable control approach.

For this case of $n = 3$ finite volume elements, the system and input matrices are given by

$$A\,(x,p) = \begin{bmatrix} a_{11} & a_{12} & 0 \\ a_{21} & a_{22} & a_{23} \\ 0 & a_{32} & a_{33} \end{bmatrix} \quad \text{and} \tag{2}$$

$$\tilde{B}\,(x,p) = \begin{bmatrix} b_{11} & b_{12} & b_{13} & b_{14} \\ b_{21} & 0 & 0 & b_{24} \\ b_{31} & 0 & 0 & b_{34} \end{bmatrix} \ , \tag{3}$$

where the state vector contains the element temperatures

$$x = \begin{bmatrix} \vartheta_{(1,1,1)} & \vartheta_{(1,2,1)} & \vartheta_{(1,3,1)} \end{bmatrix}^T \ . \tag{4}$$

Moreover, the input vector

$$\tilde{u} = \begin{bmatrix} \vartheta_{\mathrm{A}} & \vartheta_{\mathrm{AG,in}} & \vartheta_{\mathrm{CG,in}} & \frac{1}{3}I \end{bmatrix}^T \tag{5}$$

consists of the ambient temperature ϑ_{A}, the anode and cathode inlet temperatures $\vartheta_{\mathrm{AG,in}}$ and $\vartheta_{\mathrm{CG,in}}$, as well as the stack current $I_{(1,1,1)} = I_{(1,2,1)} = I_{(1,3,1)} = \frac{1}{3}I$. For a pure temperature control of the SOFC stack operated with a constant cathode gas mass flow, the only remaining control input is the cathode inlet temperature, while all other elements of $\tilde{u}$ represent measurable disturbances with respect to the state vector x. Thus, $\tilde{B}(x,p)\tilde{u}$ can be dissociated as follows

$$\tilde{B}(x,p)\tilde{u} = \underbrace{\begin{bmatrix} b_{13} \\ 0 \\ 0 \end{bmatrix}}_{B} u(t) + \underbrace{\begin{bmatrix} b_{11} & b_{12} & b_{14} \\ b_{21} & 0 & b_{24} \\ b_{31} & 0 & b_{34} \end{bmatrix}}_{E} \underbrace{\begin{bmatrix} \vartheta_{\mathrm{A}} \\ \vartheta_{\mathrm{AG,in}} \\ \frac{1}{3}I \end{bmatrix}}_{d(t)} \ . \tag{6}$$

In this paper, we restrict our attention to the design of the controller with the input $u = \vartheta_{\mathrm{CG,in}}$ when $d(t) = 0$. This assumption is motivated by neglecting heat transfer through its encasing to the ambience with temperature $\vartheta_A$and bu accounting for the fact that the anode gas enthalpy flow is smaller than the one at the cathode by more than one order of magnitude. However, extensions of the proposed method to the case of both control and disturbance inputs are straightforward in the sense of input-to-state stability (ISS) during the design procedure. Enhancing the robustness of the proposed controller by accounting for variations of the disturbance inputs will be subject of future work.

In previous work, cf. [2], [14] and the references therein, an initial identification of the matrices (2) and (3) was performed so that the interval-valued enclosure for $A\,(x,p)$ is strictly Metzler and the matrices $B\,(x,p)$ and $\tilde{B}(x,p)$ are element-wise non-negative. To obtain a reliable system model, accounting for the worst-case influence of bounded measurement tolerances on the output

$$y(t) = \begin{bmatrix} 0 & 0 & 1 \end{bmatrix} \cdot x(t) \ , \tag{7}$$

representing the outlet temperature $\vartheta_{(1,3,1)}$, as well as for possibly neglected influence of heat convection and nonlinear radiation effects, the disturbance estimation scheme summarized in the following paragraphs has been developed.

It estimates deviations between the assumed system dynamics (1) according to [2], [14] and the measured data in terms of an additive uncertainty $[\delta_i]$ for each element $i \in \{1, \ldots, n = 3\}$ of the derivative vector $\dot{x}$. This uncertainty is then mapped onto an additive interval-valued correction term for the system matrix according to

$$[A] = A\,([x],p) + \begin{bmatrix} [\delta_1] & 0 & 0 \\ 0 & [\delta_2] & 0 \\ 0 & 0 & [\delta_3] \end{bmatrix} \ , \tag{8}$$

where $A([x], p)$ represents an interval extension of the matrix A according to (2), which was evaluated in [11] for the maximum admissible range of operating temperatures, however, with purely point-valued least-squares estimates for all system parameters p. Analogously, $[\tilde{B}]$ (and its submatrix $[B]$ multiplied with the control signal u) is obtained by evaluating the respective symbolic expression for (3) over the complete range of possible temperatures. So that, we consider along the paper that the system as well as input matrices are bounded element-wise according to

$$\begin{array}{l} \underline{A} \leq A(x(t), p) \leq \overline{A} \\ 0 \leq \underline{B} \leq B(x(t), p) \leq \overline{B} \ . \end{array} \tag{9}$$

Note that the state dependencies in $A(x(t), p)$ and $B(x(t), p)$ result from a polynomial approximation of the temperature dependencies of heat capacities and reaction enthalpies of the gas fractions contained in the anode and cathode gases.

Based on (9), an interval model for (1) can be expressed as

$$\begin{array}{l} \dot{\overline{x}}(t) = \overline{A}\overline{x}(t) + \overline{B}u(t) \\ \dot{\underline{x}}(t) = \underline{A}\,\underline{x}(t) + \underline{B}u(t) \end{array} \tag{10}$$

where $\overline{x}(t)$, $\underline{x}(t) \in \mathbb{R}^n_+$ are the upper and lower bounds of the state vector; $u(t) \in \mathbb{R}^m_+$ and $y(t) \in [\underline{y}(t), \overline{y}(t)]$ are the element-wise non-negative inputs and the measurement vector with bounded uncertainty, respectively. The initial condition at the instant t_0, $x(t_0) = x_0$, is assumed to be bounded by two known upper and lower bounds according to

$$0 \leq \underline{x}_0 \leq x_0 \leq \overline{x}_0 \ . \tag{11}$$

In what follows, it is assumed that the available measurements are given by $y(t) = Cx(t)$ with additive noise $|\omega(t)| \leq \Omega$ which is unknown but restricted to the a-priori known bound $\Omega \in \mathbb{R}^p_+$ resulting in the linear output model

$$y_m(t) = Cx(t) + \omega(t) \ . \tag{12}$$

In the sequel, we are interested in designing a control law ensuring stabilization of (1) based on the interval model (10). As temperature measurements inside the stack are not available, an interval observer providing upper and lower estimates for the unknown state $x(t)$ simultaneously is built and an alternative control law is proposed by using only these interval-valued estimates.

III. Control design: an interval observer-based framework

To provide a feedback control law which can be implemented using only the interval-valued enclosures $[A]$ and $[B]$, we propose to combine the structure of a classical full state feedback controller with an interval observer in a novel fashion. The block diagram of the resulting control scheme is given in Fig. 2, where $\hat{\overline{x}}(t)$ and $\hat{\underline{x}}(t)$ are the upper and lower bounds for the estimated state trajectories. The performance requirements for the design of the controller include the following aspects:

1) The control input $u(t)$ should be designed such that the positivity of the system (1) is not violated for all $t \geq 0$, i.e., $u(t) \geq 0$;

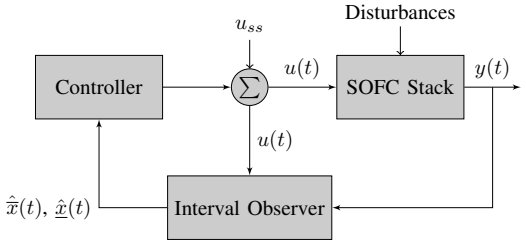

Fig. 2. Architecture of the interval observer-based state feedback control.

2) The interval inclusion

$$0 \leq \hat{\underline{x}}(t) \leq x(t) \leq \hat{\overline{x}}(t) \tag{13}$$

has to be satisfied;

3) The interval diameter $\hat{\overline{x}}(t) - \hat{\underline{x}}(t)$ has to be minimized by tuning the controller parameters;
4) The steady-state value of $\frac{\overline{x}(t)+\underline{x}(t)}{2}$ is associated with a reference input vector r consisting of the same constant elements such that

$$\frac{\overline{x}(t) + \underline{x}(t)}{2} \to r \ \text{ as } \ t \to \infty\,; \tag{14}$$

5) In order to avoid overheating phenomena of the SOFC stack, the controller must be able to prevent the stack from exceeding its maximum admissible upper temperature limit. Thus, this requirement can be described as

$$\overline{x}(t) \leq \overline{x}_{\max}, \ \ \hat{\overline{x}}(t) \leq \overline{x}_{\max} \ , \tag{15}$$

where $\overline{x}_{\max}$ is the maximum admissible temperature inside the SOFC stack.

To achieve these control objectives, the following positive interval observer is proposed

$$\left\{ \begin{array}{l} \dot{\hat{\overline{x}}}(t) = (\overline{A} - \overline{L}C)\hat{\overline{x}}(t) + \overline{B}u(t) + \overline{L}y_m(t) + \overline{L}\Omega \\ \dot{\hat{\underline{x}}}(t) = (\underline{A} - \underline{L}C)\hat{\underline{x}}(t) + \underline{B}u(t) + \max\{0, \underline{L}y_m(t) - \underline{L}\Omega\} \end{array} \right. \tag{16}$$

where $\hat{\overline{x}}(t), \hat{\underline{x}}(t) \in \mathbb{R}^n$. To preserve the order relationship (13), let $\overline{e}(t) = \hat{\overline{x}}(t) - x(t)$ and $\underline{e}(t) = x(t) - \hat{\underline{x}}(t)$ be the upper and lower estimation errors. With respect to these error vectors, we have the associated differential equations

$$\begin{array}{rl} \dot{\overline{e}}(t) = & (\overline{A} - \overline{L}C)\overline{e}(t) + (\overline{B} - B(x(t), p))u(t) \\ & + \left(\overline{A} - A(x(t), p)\right) x(t) + \overline{L}\omega(t) + \overline{L}\Omega \end{array} \tag{17}$$

and

$$\begin{array}{rl} \dot{\underline{e}}(t) = & (\underline{A} - \underline{L}C)\underline{e}(t) + (B(x(t), p) - \underline{B})\, u(t) \\ & + (A(x(t), p) - \underline{A}))\, x(t) + \underline{L}Cx(t) \\ & - \max(0, \underline{L}Cx(t) - \underline{L}(\Omega - \omega(t)) \ . \end{array} \tag{18}$$

Referring to the inequalities (9) and the fact that (1) is a positive dynamical system, i.e, $x(t) \geq 0$, $u(t) \geq 0$, then both inequalities

$$\begin{array}{l} (\overline{B} - B(x(t), p))u(t) + \left(\overline{A} - A(x(t), p)\right) x(t) \geq 0 \\ (B(x(t), p) - \underline{B})\, u(t) + (A(x(t), p) - \underline{A})\, x(t) \geq 0 \end{array} \tag{19}$$

hold. Furthermore, under the conditions $\overline{L} \geq 0$ and $\underline{L} \geq 0$, it follows that $\overline{L}\omega(t) + \overline{L}\Omega \geq 0$ and $\underline{L}Cx(t) - \max(0, \underline{L}Cx(t) -$

$\underline{L}(\Omega-\omega(t)) \geq 0$. Moreover, if $(\overline{A}-\overline{L}C)$ and $(\underline{A}-\underline{L}C)$ are chosen to be Metzler matrices, then, the inclusion property (13) is satisfied provided that (11) is also satisfied.
Now, consider the following interval observer-based controller

$$u(t) = \overline{K}(\hat{\overline{x}}(t) - \overline{x}_{ss}) + \underline{K}(\hat{\underline{x}}(t) - \underline{x}_{ss}) + u_{ss} \ , \tag{20}$$

where $u_{ss} = N_u r$, $\overline{x}_{ss} = \overline{N}_x r$ and $\underline{x}_{ss} = \underline{N}_x r$. $\overline{N}_x$, $\underline{N}_x$, N_u, $\overline{K}$, $\underline{K} \in \mathbb{R}^{m\times n}$ are the observer-based controller gains to be designed. Define $\xi(t) = \begin{bmatrix}\overline{x}^T(t) & \underline{x}^T(t) & \hat{\overline{x}}^T(t) & \hat{\underline{x}}^T(t)\end{bmatrix}^T$. Combining the open-loop model (10) as well as the positive interval observer (16) and substituting $u(t)$ by (20) for $r = 0$ yield the $4n$-dimensional closed-loop system

$$\begin{bmatrix}\dot{\overline{x}}(t)\\ \dot{\underline{x}}(t)\\ \dot{\hat{\overline{x}}}(t)\\ \dot{\hat{\underline{x}}}(t)\end{bmatrix} = \begin{bmatrix}\overline{A} & 0 & \overline{B}\,\overline{K} & \overline{B}\underline{K}\\ 0 & \underline{A} & \underline{B}\overline{K} & \underline{B}\underline{K}\\ 0 & 0 & \overline{A}-\overline{L}C+\overline{B}\,\overline{K} & \overline{B}\,\underline{K}\\ 0 & 0 & \underline{B}\overline{K} & \underline{A}-\underline{L}C+\underline{B}\,\underline{K}\end{bmatrix} \cdot \begin{bmatrix}\overline{x}(t)\\ \underline{x}(t)\\ \hat{\overline{x}}(t)\\ \hat{\underline{x}}(t)\end{bmatrix} + \begin{bmatrix}0\\ 0\\ \overline{L}y_m(t)+\overline{L}\Omega\\ \max\{0, \underline{L}y_m(t)-\underline{L}\Omega\}\end{bmatrix} . \tag{21}$$

With the help of the abbreviations

$$\mathbb{A} = \begin{bmatrix}\overline{A} & 0\\ 0 & \underline{A}\end{bmatrix}, \mathbb{B} = \begin{bmatrix}\overline{B}\\ \underline{B}\end{bmatrix}, \mathbb{K} = \begin{bmatrix}\overline{K} & \underline{K}\end{bmatrix} \mathbb{C} = \begin{bmatrix}C & 0\\ 0 & C\end{bmatrix},$$
$$\mathbb{L} = \begin{bmatrix}\overline{L} & 0\\ 0 & \underline{L}\end{bmatrix}, \mathbb{D}(t) = \begin{bmatrix}0\\ 0\\ \overline{L}y_m(t)+\overline{L}\Omega\\ \max\{0, \underline{L}y_m(t)-\underline{L}\Omega\}\end{bmatrix},$$

equation (21) is rewritten into

$$\dot{\xi}(t) = \begin{bmatrix}\mathbb{A} & \mathbb{B}\mathbb{K}\\ 0 & \mathbb{A}-\mathbb{L}\mathbb{C}+\mathbb{B}\mathbb{K}\end{bmatrix}\xi(t) + \mathbb{D}(t) \ . \tag{22}$$

For stability analysis, we consider the block-diagonal quadratic ISS-Lyapunov function of the form

$$V(\xi(t)) = \xi^T(t)P\xi(t) = \xi^T(t)\begin{bmatrix}\mathbb{P}_1 & 0\\ 0 & \mathbb{P}_2\end{bmatrix}\xi(t) \ , \tag{23}$$

where $\mathbb{P}_1$ and $\mathbb{P}_2$ are diagonal positive matrices.
Taking the time derivative of the Lyapunov function (23) along the trajectory of the closed-loop system (22), we get

$$\dot{V}(\xi(t)) = \xi^T(t)\Bigg(\begin{bmatrix}\mathbb{A} & \mathbb{B}\mathbb{K}\\ 0 & \mathbb{A}-\mathbb{L}\mathbb{C}+\mathbb{B}\mathbb{K}\end{bmatrix}^T P + P\begin{bmatrix}\mathbb{A} & \mathbb{B}\mathbb{K}\\ 0 & \mathbb{A}-\mathbb{L}\mathbb{C}+\mathbb{B}\mathbb{K}\end{bmatrix}\Bigg)\xi(t) + \mathbb{D}^T P\xi(t) + \xi^T(t)P\mathbb{D}(t) . \tag{24}$$

Let γ and ε be two positive scalars. Then, by adding and subtracting the terms $\varepsilon\xi^T(t)P\xi(t)$ and $-\gamma\ \mathbb{D}^T(t)\ \mathbb{D}(t)$, (24) becomes

$$\begin{aligned}&\dot{V}(\xi(t)) = \begin{bmatrix}\xi^T(t) & \mathbb{D}^T(t)\end{bmatrix}^T \Phi \begin{bmatrix}\xi(t) & \mathbb{D}(t)\end{bmatrix}^T\\ &-\varepsilon V(\xi(t)) + \gamma\mathbb{D}^T(t)\mathbb{D}(t)\end{aligned} \tag{25}$$

with

$$\Phi = \left[\begin{array}{cc:c}\begin{bmatrix}\mathbb{A} & \mathbb{B}\mathbb{K}\\ 0 & \mathbb{A}-\mathbb{L}\mathbb{C}+\mathbb{B}\mathbb{K}\end{bmatrix}^T P + & & \\ P\begin{bmatrix}\mathbb{A} & \mathbb{B}\mathbb{K}\\ 0 & \mathbb{A}-\mathbb{L}\mathbb{C}+\mathbb{B}\mathbb{K}\end{bmatrix} + \varepsilon P & & P\\ \hdashline & P & -\gamma\mathcal{I}_{4n}\end{array}\right] .$$

If the gain matrices $\mathbb{K}$ and $\mathbb{L}$ are found such that

$$\Phi \prec 0 \tag{26}$$

is satisfied, the inequality

$$\dot{V}(\xi(t)) < -\varepsilon V(\xi(t)) + \gamma\mathbb{D}^T(t)\mathbb{D}(t) \tag{27}$$

holds. Multiplying both sides of (27) by $e^{\varepsilon t}$ and integrating from 0 to t, one obtains

$$V(\xi(t)) < -V(0)e^{-\varepsilon t} + \gamma\int_0^t e^{-\varepsilon(t-s)}\|\mathbb{D}(s)\|_2^2 \mathrm{d}s \ . \tag{28}$$

Recall that for any $\xi(t) \in \mathbb{R}^{4n}$, the bounds

$$\varepsilon_1\|\xi(t)\|_2^2 \leq V(\xi(t)) \leq \varepsilon_2\|\xi(t)\|_2^2, \ \ \forall\xi(t) \in \mathbb{R}^{4n} \tag{29}$$

hold, where

$$\varepsilon_1 = \lambda_{\min}(P), \ \ \varepsilon_2 = \lambda_{\max}(P) \tag{30}$$

in which $\lambda_{\min}(P)$ and $\lambda_{\max}(P)$ denote the minimal and maximal eigenvalue of the matrix P, respectively. Then, the inequality (28) becomes

$$\|\xi(t)\|_2^2 \leq \frac{\varepsilon_2}{\varepsilon_1}\|\xi(0)\|_2^2 e^{-\varepsilon t} + \frac{\gamma}{\varepsilon\varepsilon_1}\|\mathbb{D}(t)\|_\infty^2 \tag{31}$$

leading to

$$\|\xi(t)\|_2 \leq \sqrt{\frac{\varepsilon_2}{\varepsilon_1}}\|\xi(0)\|_2 e^{-\frac{\varepsilon}{2}t} + \sqrt{\frac{\gamma}{\varepsilon\varepsilon_1}}\|\mathbb{D}(t)\|_\infty \tag{32}$$

which implies that the system (22) is ISS if (26) is satisfied. The radius of the convergence region is upper bounded by $\sqrt{\frac{\gamma}{\varepsilon\varepsilon_1}}\|\mathbb{D}(t)\|_\infty^2$. Thus, the bilinear matrix inequality (BMI) (26) can be used to construct the optimal solution by minimization of $\gamma \geq 0$.
Although the proposed observer-based state feedback approach provides a controller that minimizes the norm of the disturbances, the state constraint (15) has not been taken into consideration yet. Let us consider the Lyapunov level set

$$\Omega(P) = \{\xi(t) \in \mathbb{R}^{4n} \big| \xi^T(t)P\xi(t) \leq 1\} \ , \tag{33}$$

which is positively invariant with respect to the motion of the closed-loop system (22) (i.e., for every initial condition $\xi(0)$ inside $\Omega(P)$ the trajectory of $\xi(t)$ remains in $\Omega(P)$ for all $t \geq 0$). Now, define the following set of state constraints

$$\mathcal{L}(F, \vartheta) = \{\xi(t) \in \mathbb{R}^{4n} \big| F\xi(t) \leq \vartheta\} \ , \tag{34}$$

where $F \in \mathbb{R}^{q\times 4n}$ and $\vartheta \in \mathbb{R}^q$ are given. According to the previous considerations, if $\Omega(P) \subset \mathcal{L}(F, \vartheta)$ and P satisfies the condition (26), then for any initial condition inside the ellipsoid $\Omega(P)$ we have $\xi(t) \in \mathcal{L}(F, \vartheta)$ for all $t \geq 0$. From [10], we obtain the following useful Lemma.

Lemma 1. [10] The inclusion $\Omega(P) \subset \mathcal{L}(F, \vartheta)$ is equivalent to the existence of positive scalars $a_1, \ldots, a_q > 0$ such that

$$\begin{bmatrix}4a_i\vartheta_i - F_iP_iF_i^T & 2a_i\\ 2a_i & 1\end{bmatrix} \geq 0 \ , \ \ \forall i \in \{1, \ldots, q\} \ , \tag{35}$$

where F_i is the i^{th} row of F.

Remark. Regarding the result above, the state set (34) satisfying the constraints (15) can be chosen as

$$F = \begin{bmatrix}\mathbb{1}_n & 0 & 0 & 0\\ 0 & 0 & \mathbb{1}_n & 0\end{bmatrix}, \ \vartheta = \begin{bmatrix}\overline{x}_{\max}\\ \overline{x}_{\max}\end{bmatrix} \ . \tag{36}$$

The following theorem summarizes the discussion above. The operators ">", "$\geq$" are applied element-wise.

Theorem 1. The control law $u(t)$ given in (20) with $r = 0$ is robustly stabilizing in an ISS sense, if there exist positive diagonal matrices $\mathbb{P}_1$, $\mathbb{P}_2$, and $\mathbb{P}_3$, full matrices $\mathbb{W}$ and $\mathbb{Y}$, scalars $\gamma > 0$, $a_1, \ldots, a_q > 0$ for given ε, $\eta \in \mathbb{R}_+$, $F \in \mathbb{R}^{q \times 4n}$, and $\vartheta \in \mathbb{R}^q$ such that the following LMIs hold true,

$$\min_{\mathbb{P}_1, \mathbb{P}_2, \mathbb{P}_3, \mathbb{W}, \mathbb{Y}, a_1, \ldots, a_q} \quad \gamma$$

$$\mathbb{W} > 0 \ , \tag{37a}$$

$$\mathbb{Y} > 0 \ , \tag{37b}$$

$$\mathbb{P}_2 \mathbb{A} - \mathbb{Y}\mathbb{C} + \eta \mathbb{P}_2 \geq 0 \ , \tag{37c}$$

$$\mathbb{P}_2 \mathbb{B} = \mathbb{B} \mathbb{P}_3 \ , \tag{37d}$$

$$\begin{bmatrix} 4a_i\vartheta_i - F_i P_i F_i^T & 2a_i \\ 2a_i & 1 \end{bmatrix} \geq 0, \ \ \forall i \in \{1, \ldots, 4n\} \ , \tag{37f}$$

where $\mathbb{L} = \mathbb{P}_2^{-1}\mathbb{Y}$ and $\mathbb{K} = \mathbb{P}_3^{-1}\mathbb{W}$.

Proof. The element-wise inequality (37a) guarantees the positivity of the controller gains, (i.e., $\overline{K} \geq 0$ and $\underline{K} \geq 0$), and therefore, the positivity of the control law $u(t)$. Moreover, the element-wise inequality (37b) ensures the positivity of the interval observer gains. Furthermore, from [5], the matrices $(\overline{A} - \overline{L}C)$ and $(\underline{A} - \underline{L}C)$ are Metzler if and only if there exists a positive scalar η such that

$$(\mathbb{A} - \mathbb{L}\mathbb{C}) + \eta \mathcal{I}_{2n} \geq 0 \ . \tag{38}$$

Multiplying the left-hand side of (38) by $\mathbb{P}_2$ together with the change of coordinates $\mathbb{Y} = \mathbb{P}_2\mathbb{L}$, (37c) is directly obtained. The LMI (37f) guarantees the inclusion of the ellipsoid $\Omega(P)$ in the set of trajectories $\mathcal{L}(F, \vartheta)$. According to (26), the LMIs (37d) and (37e) guarantee ISS stability of the closed-loop system (22). After some calculations, the BMI (26) is rewritten into

$$\left[\begin{array}{cc|cc} \mathbb{P}_1\mathbb{A} + \mathbb{A}^T\mathbb{P}_1 + \varepsilon\mathbb{P}_1 & \mathbb{P}_2\mathbb{B}\mathbb{K} & \mathbb{P}_1 & 0 \\ \mathbb{K}^T\mathbb{B}^T\mathbb{P}_2 & \Xi & 0 & \mathbb{P}_2 \\ \hline & & & \\ \multicolumn{2}{c|}{\begin{matrix} \mathbb{P}_1 & 0 \\ 0 & \mathbb{P}_2 \end{matrix}} & \multicolumn{2}{c}{-\gamma\mathcal{I}_{4n}} \end{array}\right] \prec 0,$$

where $\Xi = \mathbb{P}_2\mathbb{A} + \mathbb{A}^T\mathbb{P}_2 + \varepsilon\mathbb{P}_2 - \mathbb{P}_2\mathbb{L}\mathbb{C} - \mathbb{C}^T\mathbb{L}^T\mathbb{P}_2 + \mathbb{P}_2\mathbb{B}\mathbb{K} + \mathbb{K}^T\mathbb{B}^T\mathbb{P}_2$. To deal with the bilinear term $\mathbb{P}_2\mathbb{B}\mathbb{K}$, the equality (37d) is introduced. Then, by letting $\mathbb{W} = \mathbb{P}_3\mathbb{K}$ and $\mathbb{Y} = \mathbb{P}_2\mathbb{L}$, (37e) is obtained. This completes the proof. □

Finally, it is desired that the mean value $\frac{\overline{x}(t)+\underline{x}(t)}{2}$ tracks a reference input r such that $\frac{\overline{x}(t)+\underline{x}(t)}{2} \to r$ as $t \to \infty$. To find $\overline{N}_x$, $\underline{N}_x$, and N_u, we consider the desired steady-state relationships:

$$\begin{aligned} &\dot{\overline{x}}_{ss} = \overline{A}\overline{x}_{ss} + \overline{B}u_{ss} = (\overline{A}\,\overline{N}_x + \overline{B}N_u)r = 0 \\ &\dot{\underline{x}}_{ss} = \underline{A}\,\underline{x}_{ss} + \underline{B}u_{ss} = (\underline{A}\,\underline{N}_x + \underline{B}N_u)r = 0 \\ &\begin{bmatrix} \frac{1}{2}\mathcal{I}_n & \frac{1}{2}\mathcal{I}_n \end{bmatrix} \begin{bmatrix} \overline{x}_{ss} \\ \underline{x}_{ss} \end{bmatrix} = \begin{bmatrix} \frac{1}{2}\overline{N}_x & \frac{1}{2}\underline{N}_x \end{bmatrix} \begin{bmatrix} \mathbb{1}_n \\ \mathbb{1}_n \end{bmatrix} r = r \ . \end{aligned} \tag{39}$$

Thus, the possible solutions can be found by solving the following set equality constraints

$$\begin{bmatrix} \overline{A} & 0 & \overline{B} \\ 0 & \underline{A} & \underline{B} \\ \frac{1}{2}\mathcal{I}_n & \frac{1}{2}\mathcal{I}_n & 0 \end{bmatrix} \begin{bmatrix} \overline{N}_x \\ \underline{N}_x \\ N_u \end{bmatrix} = \begin{bmatrix} 0 \\ 0 \\ 1 \end{bmatrix} \ . \tag{40}$$

Finally, the control law (20) is equivalent to

$$u(t) = \overline{K}\hat{\overline{x}}(t) + \underline{K}\,\hat{\underline{x}}(t) + (N_u - \overline{K}\,\overline{N}_x - \underline{K}\,\underline{N}_x)r \ . \tag{41}$$

Thus, to ensure that $u(t)$ remains positive, the matrix $(N_u - \overline{K}\,\overline{N}_x - \underline{K}\underline{N}_x)$ should be positive element-wise according to

$$\begin{bmatrix} -\overline{K} & -\underline{K} & 1 \end{bmatrix} \begin{bmatrix} \overline{N}_x \\ \underline{N}_x \\ N_u \end{bmatrix} \geq 0 \ . \tag{42}$$

Therefore, the steady-state controller design can be achieved by satisfying the linear constraints (40), (42).

IV. Application to Robust Temperature Control of an SOFC Stack

The dynamic model according to Sec. II used for the interval observer-based control design has been validated using real measured data gathered during the heating phase of an SOFC stack module available at the Chair of Mechatronics at the University of Rostock with the parameters $L = N = 1$ and $M = 3$.

The observer-based controller gains $\overline{K}$, $\underline{K}$, $\overline{L}$, and $\underline{L}$ are obtained by solving the convex optimization problem in Theorem 1 with $C = \begin{bmatrix} 0 & 0 & 1 \end{bmatrix}$, $\overline{x}_{\max} = 1000\,\mathrm{K}$, $\varepsilon = 0.5$ and $\eta = 0.25$. The measurement tolerance Ω is taken to be equal to $15\,\mathrm{K}$. By applying Theorem 1, the following gains are obtained

$$\begin{aligned} \overline{L} &= \begin{bmatrix} 0.0000 \\ 0.0036 \\ 0.1808 \end{bmatrix}, \ \underline{L} = \begin{bmatrix} 0.0000 \\ 0.0035 \\ 0.1686 \end{bmatrix} \\ \overline{K} &= \begin{bmatrix} 0.0156 & 0.0134 & 0.0864 \end{bmatrix}, \\ \underline{K} &= \begin{bmatrix} 0.0199 & 0.0175 & 0.1078 \end{bmatrix}, \\ N_u = 0.9388, \ \overline{N}_x &= \begin{bmatrix} 1.0448 \\ 1.1306 \\ 1.1641 \end{bmatrix}, \ \underline{N}_x = \begin{bmatrix} 0.9552 \\ 0.8783 \\ 0.7214 \end{bmatrix} \end{aligned}$$

with $\gamma = 10^{-5}$.

Corresponding simulation results are depicted in Figs. 3 and 4. From these results, it can be concluded that the robust state feedback control design has been achieved successfully under consideration of the predefined state constraints. Furthermore, the estimates provided by the interval observer approach the desired steady-state operating point ($r = 750\,\mathrm{K}$). It should be noted that the reason why the average value of these estimates does not reach exactly the desired reference value r is because the dimension of the state space is greater than the number of control inputs ($n = 3$, $m = 1$) which reveals the under-actuated character of the system.

V. Conclusions and Outlook on Future Work

The novel interval observer-based state feedback controller presented in this paper allows for preventing the violation of state constraints for dynamic systems given in the form of linear, cooperative ODEs with interval-bounded parameter

$$\left[\begin{array}{cc|cc} \mathbb{P}_1\mathbb{A}+\mathbb{A}^T\mathbb{P}_1+\varepsilon\mathbb{P}_1 & \mathbb{B}\mathbb{W} & \mathbb{P}_1 & 0 \\ \mathbb{W}^T\mathbb{B}^T & \mathbb{P}_2\mathbb{A}+\mathbb{A}^T\mathbb{P}_2+\varepsilon\mathbb{P}_2-\mathbb{Y}\mathbb{C}-\mathbb{C}^T\mathbb{Y}^T+\mathbb{B}\mathbb{W}+\mathbb{W}^T\mathbb{B}^T & 0 & \mathbb{P}_2 \\ \hline & & \multicolumn{2}{c}{\multirow{2}{*}{$-\gamma\mathcal{I}_{4n}$}} \\ & & \mathbb{P}_1 & 0 \\ & & 0 & \mathbb{P}_2 \end{array}\right] \prec 0 \ , \tag{37e}$$

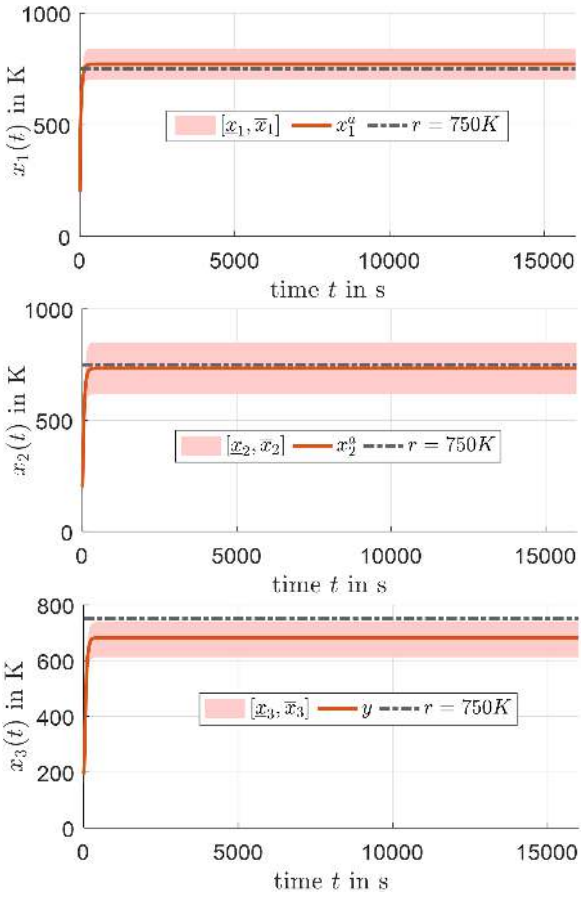

Fig. 3. Time evolution of the upper and lower estimates of the states x_1, x_2 and x_3 with their average values.

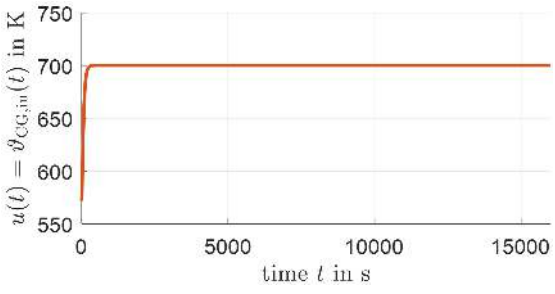

Fig. 4. Time evolution of the control action.

uncertainty. The applicability of the controller is demonstrated in simulations for the thermal behavior of a high-temperature SOFC stack, allowing for preventing overshooting safety-critical temperature bounds in a reliable manner.

Future work will extend this research by accounting for the neglected disturbances in (6) and the dynamics of actuators (e.g., the lag behavior of the preheaters of the SOFC) in combination with corresponding range constraints for the admissible control signals and their admissible variation rates. Moreover, possibilities for the reduction of the control and observation effort by the development of partial state feedback controllers or pure output feedback strategies will be further investigated.

REFERENCES

[1] R. Bove and S. Ubertini, editors. *Modeling Solid Oxide Fuel Cells*. Springer, Berlin, 2008.

[2] Th. Dötschel, E. Auer, A. Rauh, and H. Aschemann. Thermal Behavior of High-Temperature Fuel Cells: Reliable Parameter Identification and Interval-Based Sliding Mode Control. *Soft Computing*, 17(8):1329–1343, 2013.

[3] D. Efimov, T. Raïssi, S. Chebotarev, and A. Zolghadri. Interval State Observer for Nonlinear Time Varying Systems. *Automatica*, 49(1):200–205, 2013.

[4] D. Ichalal, B. Marx, D. Maquin, and J. Ragot. State Estimation of System with Bounded Uncertain Parameters: Interval Multimodel Approach. *International Journal of Adaptive Control and Signal Processing*, 32:480–493, 2018.

[5] S. Ifqir, D. Ichalal, N. Ait Oufroukh, and S. Mammar. Robust Interval Observer for Switched Systems with Unknown Inputs: Application to Vehicle Dynamics Estimation. *European Journal of Control*, 44:3–14, 2018.

[6] T. Kaczorek. *Positive 1D and 2D Systems*. Springer–Verlag, London, 2002.

[7] T. Kharkovskaya, D. Efimov, A. Polyakov, and J.-P. Richard. Design of Interval Observers and Controls for PDEs Using Finite-Element Approximations. *Automatica*, 93:302–310, 2018.

[8] J.T. Pukrushpan, A.G. Stefanopoulou, and H. Peng. *Control of Fuel Cell Power Systems: Principles, Modeling, Analysis and Feedback Design*. Springer, Berlin, 2nd edition, 2005.

[9] T. Raïssi and D. Efimov. Some Recent Results on the Design and Implementation of Interval Observers for Uncertain Systems. *at-Automatisierungstechnik*, 66(3):213–224, 2018.

[10] M. Ait Rami, H. Ayad, and F. Mesquine. Enlarging Ellipsoidal Invariant Sets for Constrained Linear Systems. *International Journal of Innovative Computing, Information and Control*, 3(5):1097–1108, 2007.

[11] A. Rauh, J. Kersten, and H. Aschemann. An Interval Observer Approach for the Online Temperature Estimation in Solid Oxide Fuel Cell Stacks. In *2018 European Control Conference (ECC)*, pages 1596–1601. IEEE, 2018.

[12] A. Rauh, L. Senkel, and H. Aschemann. Interval-Based Sliding Mode Control Design for Solid Oxide Fuel Cells with State and Actuator Constraints. *IEEE Transactions on Industrial Electronics*, 62(8):5208–5217, 2015.

[13] A. Rauh, L. Senkel, and H. Aschemann. Reliable Sliding Mode Approaches for the Temperature Control of Solid Oxide Fuel Cells with Input and Input Rate Constraints. In *Proceedings of 1st IFAC Conference on Modelling, Identification and Control of Nonlinear Systems, MICNON 2015*, St. Petersburg, Russia, 2015.

[14] A. Rauh, L. Senkel, J. Kersten, and H. Aschemann. Reliable Control of High-Temperature Fuel Cell Systems Using Interval-Based Sliding Mode Techniques. *IMA Journal of Mathematical Control and Information*, 33(2):457–484, 2014.

[15] H.L. Smith. *Monotone Dynamical Systems: An Introduction to the Theory of Competitive and Cooperative Systems*. Number 41. American Mathematical Soc., 2008.